Application of a hybrid collisional radiative model to recombining argon plasmas

J. Quant. Spectrosc. Radiat. Transfer Vol. 49, No. 2, pp. 129–139, 1993
Printed in Great Britain.

0022-4073/93 $6.00 + 0.00

APPLICATION OF A HYBRID COLLISIONAL RADIATIVE MODEL TO RECOMBINING ARGON PLASMAS

D. A. BENOY, J. A. M. VAN DER MULLEN,† M. C. M. VAN DE SANDEN, B. VAN DER SIJDE, and D. C. SCHRAM
Physics Department, Eindhoven University of Technology, P.O. Box 513, 5600 MB Eindhoven, The Netherlands

(Received 13 April 1992)

Abstract—A collisional radiative model, in which a hybrid cut-off technique is used, is applied to recombining plasmas to study the atomic state distribution (ASDF) and the recombination coefficient. Computations of the ASDF using semi-empirical rate coefficients of Vriens and Smeets (V–S) and Drawin (D) are compared with experimental values measured at various positions in a free expanding argon arc jet. Apart from the shock position, where the calculated results are too low, the model calculations are higher than the experimental results. The volumetric recombination coefficient has a $T_e^{-4.2}$ and a $T_e^{-4.8}$ dependence when semi-empirical rate coefficients of, respectively, V–S and D are used. The differences between the models based on the rate coefficients of V–S and D indicate that the recombination flow is sensitive to the low temperature behavior of the rate coefficients.

1. INTRODUCTION

Knowledge of the atomic state distribution function (ASDF) is of fundamental importance in the field of plasma spectroscopy, recombination lasers, plasma-transport models, astrophysics, and the study of impurities in thermonuclear plasmas. The ASDF describes how excited states in atoms and ions are populated in relation to a given electron temperature T_e, neutral ground-state density n_1 and electron density n_e. With this function it is possible to calculate the coefficients of total recombination and ionization,[1] which are required for the particle- and energy source terms in plasma-transport equations.[2] At present, there is no general analytical solution for the ASDF under various conditions. On the contrary, several calculations exist for specific density and temperature ranges where various sets of semi-empirical expressions for the cross sections related to electron induced transistions are used.

In a recent paper of Benoy et al[3] a new technique was developed in which the analytical solution for the upper part of atomic systems can be used to simplify the numerical part of the ASDF of argon drastically. This so-called hybrid technique based on a combination of analytical and numerical techniques, as described by van der Mullen,[4] makes it possible to reduce the number of atomic levels needed in a numerical model drastically.[5] As a result the computational effort is minimized so that the hybrid technique is very suitable for the source terms in transport models. Moreover, it is a practical method for a comparative study of ASDFs generated by different sets of semi-empirical rate coefficients.

In Ref. 3 the hybrid technique has been applied to conditions corresponding to ionizing plasma regions.[6,7,8] In the present paper, the characteristics of a recombining argon plasma are studied using two different hybrid CR-models which differ from each other with respect to the set of semi-empirical rates. One of the models is based on formulae published by Vriens and Smeets[9] and the other uses the rates as given by Drawin.[10] In both cases the ASDF as well as the recombination coefficients are calculated. The result of both hybrid models will be compared with experimental results obtained from a cascaded, arc-created expanding plasma. The comparative study will reveal substantial differences between the two different models with respect to the ASDF as well as the coefficient of total recombination. This is essentially based on the fact that the kinetics of a cold

†To whom all correspondence should be addressed.

recombining plasma is determined by the unknown threshold behavior of electron collisions. The experimental results are not suitable for selecting one of the sets of semi-empirical rate coefficients.

We will start with an outline of the hybrid technique.

2. THE HYBRID CUT-OFF TECHNIQUE

2.1. The general set-up of the collisional-radiative models

The calculation of the two different sets of ASDFs is done using numerical collisional-radiative (CR) models, as initiated by Bates et al.[11] The number of levels used in the CR models is reduced drastically by providing the cut-off level with a stepwise ionization/recombination flow as prescribed in Ref. 4 and worked out in Ref. 3 for an ionizing argon system. The construction of a model in which the lower part of the atomic system is calculated numerically while the upper part obeys an analytical relation, is denoted by the hybrid model. This will be described in Sec. 2.2. This section is devoted to the general set up for CR models.

Under a quasi-steady state (QSS), i.e. when the CR-relaxation times for excited levels ($10^{-7} \sim 10^{-8}$ sec) are much shorter than the hydrodynamical relaxation times ($10^{-3} \sim 10^{-4}$ sec), the equation for the population density $n(p)$ for excited levels reads

$$\left.\frac{\partial n(p)}{\partial t}\right|_{\mathrm{CR}} = 0, \quad p > 1. \tag{1}$$

The symbol p is used to number the levels in an atomic system or it represents the effective principal quantum number (pqn).[4] The densities n_1, n_+, the electron density n_e and the electron temperature T_e, which are the main input parameters for CR-models, follow from the experiment[6,7,8] or from plasma-transport models. The following CR processes are considered in the CR-models: electron-heavy particle inelastic collisions, line radiations and radiative recombination. The absorption of resonant radiation and the photo-ionization are described with an escape factor. The effect of stimulated emission and inelastic collisions induced transitions, a Maxwellian electron energy distribution function (EEDF) is used. The argon system of levels being used is described in Ref. 3. As stated before, we will construct two different CR models which only differ with respect to the rate of excitation processes of excited levels. The model denoted by V uses the rates of Vriens and Smeets[9] whereas model D is based on cross sections of Drawin.[10] In these semi-empirical expressions, known values for the optical transition probabilities of Wiese et al[12] or hydrogenlike values are implemented.[4] The remaining part of the models are the same. Experimental data of Tachibana are used for the ground-state excitation,[13] whereas the escape factor for radiative transitions to the ground-state employs a model of Klein.[14] For all other radiative transitions, the plasma is taken to be optically thin. For radiative recombination we use data of Katsonis.[15]

The population density of an excited level $p(2, \ldots, N)$ can be described by the following equation:

$$\sum_{q>1}^{N} C_{qp} n(q) = n_+ C_{+p} + n_1 C_{1p}. \tag{2}$$

The coefficients C_{qp} are known functions of the rate coefficients, T_e, n_e, and escape factors. The solution of Eq. (2) can be written in standard form, i.e. in terms of a ground-state $n^1(p)$ and an ion contribution $n^+(p)$, since Eq. (2) is a linear set of equations, viz.,

$$n(p) = n^+(p) + n^1(p). \tag{3}$$

It is convenient to relate the ground-state contribution to the corresponding Boltzmann population $n^B(p)$, $n^1(p) = r^1(p) n^B(p)$ and the ion contribution to the corresponding Saha population $n^S(p)$, $n^+(p) = r^+(p) n^S(p)$, where

$$\frac{n^B(p)}{g_p} = \frac{n_1}{g_1} \exp(-E_{1p}/kT_e), \tag{4}$$

$$\frac{n^S(p)}{g_p} = \frac{n_e n_+}{2g_+} \left(\frac{h^2}{2\pi m_e kT_e}\right)^{3/2} \exp(E_{p+}/kT_e). \tag{5}$$

In these formulae, E_{1p} is the excitation energy, E_{p+} the ionization energy of level p and g_p the statistical weight of level p. The coefficients $r^+(p)$ and $r^1(p)$ are the population coefficients for a purely recombining and ionizing plasma, respectively. Another instructive expression for the excited state population density is obtained when Eq. (3) is divided by $n^S(p)$, i.e.

$$b(p) = r^+(p) + r^1(p)b(1), \tag{6}$$

where $b(p) = n(p)/n^S(p)$. A level p is said to be over or under-populated with respect to Saha when $b(p) > 1$ or $b(p) < 1$, respectively.

2.2. The cut-off procedure

An important method to simplify a CR-model is the reduction of the number of levels. In the model of Bates et al[11] a cut-off of the atomic system is used at a level which is supposed to be in Saha equilibrium. Because of the increasing collisional rate coefficients for ionization and recombination for increasing p values, the higher levels in atomic or ionic system reach Saha equilibrium more easily than the lower levels. A level p and all higher-lying levels are said to be in partial local Saha equilibrium (pLSE) if they are populated according to Eq. (5) which is equivalent to $b(p) = 1$. However, such a level can be very high in the atomic system so that the number of levels to be treated in the CR-model must be large. Moreover, small deviations from the Saha density as given by Eq. (5) may cause large excitation flows in the upper part of the system which will effect the ionization or recombination coefficients and thus the density of lower levels. This is due to the fact that the rate coefficient for stepwise excitation scales with p.[4]

The discussion of finding the lowest level in pLSE is often guided by the Griem criterion[16] which states that for a level p in pLSE the total collisional depopulation should be larger than the total radiative depopulation. This condition defines a critical level p_{cr} dependent on n_e which is a boundary level between the radiative and collisional dominated part of the atomic system. Explicit expressions for p_{cr} have been derived for hydrogen like systems in Refs. 17, 18. However, although Griem's condition is nearly always needed, it is hardly ever sufficient for the presence of pLSE. There are two situations in which the incompleteness of this condition can be demonstrated. First, as can be seen from Eq. (5), $b(p)$ depends on the magnitude of $b(1)$, so that when $b(1) \gg 1$ in an ionizing plasma, the excited level populations are governed by the ground-state population. Apart from an n_e criterion, n_1 must also be specified. The second situation deals with cold recombining systems where, although $b(1) \ll 1$, even large n_e-values can not prevent that the ASDF differs substantially from the Saha value. This result is caused by the fact that for low T_e-values, the deexcitation of lower levels supercedes excitation due to the fact that electrons are missing sufficient translational energy for excitation.[16] The result implies that apart from n_e and $b(1)$, we must also put a demand on the T_e-value in order to mark out the validity regime of pLSE. This T_e-related boundary condition can be obtained by the requirement that for the boundary level the excitation process $p \to p + 1$ has the same probability as the deexcitation process $p \to p - 1$, which leads to the so called hot–cold boundary level[19]

$$p_{hc} = Z\sqrt{Ry/kT_e\,\delta}, \tag{7}$$

where Ry is the Rydberg energy and δ represents a parameter which depends on the atomic system and the adopted theory. For hydrogen-like systems, Biberman et al prescribe $\delta = 1.52$;[20] in the model of Mansbach and Keck, $\delta = 3.83$;[21] in the work of Fujimoto, $\delta = 3$.[1,19]

When Griem's condition and $p > p_{hc}$ are fulfilled, the system is ruled by the so-called (de)excitation saturation balance (DSB/ESB) and is dominated by stepwise processes. This stepwise (de)excitation flow over collision-dominated excited levels can be described analytically both for ionizing and recombining systems. The change of the excitation flow over the system of levels can be described using a continuity equation in excitation space.[4] The difference between the recombining and ionising case is then reduced to a difference in boundary condition. In both cases it can be shown that the Saha decrement $\delta b(p) = b(p) - 1$ scales with $|\delta b(p)| \sim p^{-6}$ which means for the ionizing case that[4,17]

$$\delta b(p) \simeq r^1(p)\delta b(1) \sim p^{-6}. \tag{8}$$

On the other hand, for recombining systems, the relation

$$-\delta b(p) \simeq 1 - r^{+}(p) \sim p^{-6} \tag{9}$$

holds. This is closely related to the fact that for sufficiently large n_e-values, the superposition of ionization and recombination flows of the same magnitude gives the relation $r^{1}(p) + r^{+}(p) = 1$, which is the so-called complementary property of $r^{1}(p)$ and $r^{+}(p)$.[4,24] In the hybrid cut-off technique, the analytical expressions (8) and (9) are used for the cut-off level to construct the (de)-excitation flow. This provides the coupling of the highest level with the continuum. In ionizing systems, this is the stepwise ionization while in recombining systems it is the stepwise recombination. It should be noted that in the hybrid cut-off technique an excitation flow is used as boundary condition rather than a population density as in Ref. 11. The principal quantum number at cut-off N in Eq. (2) should be at least $N \geqslant \max(p_{hc}, p_{cr})$. This number is much smaller than that prescribed by the method of Bates et al.[11] In the CR-models for Ar of Katsonis[15] and Vlček and Pelikán,[22] cut-off principal quantum numbers of 50 and 19 are used, respectively, while in our CR-model $N = 13$. Depending on the conditions the number of levels can even be reduced. In Sec. 4, the hybrid cut-off technique is compared with the technique proposed in Ref. 11. We shall call the technique in which the cut-off level N has only an ionization recombination channel a *stagnation* cut-off. The reason is that when $b(N) \neq 1$ the excitation current is obstructed. For obvious reasons, we will denote the new technique as the *conductive* cut-off.

3. CASCADED ARC CREATED EXPANDING PLASMA

In Ref. 3 the hybrid cut-off technique has been applied to specific (ionizing) plasma conditions according to the work of van der Mullen.[4,7,8] This study is focussed on recombining systems which can be found in non-current carrying plasmas or plasma regions such as afterglows, outer regions of flames,[6] recombination lasers and so on. Our main attention goes to the recombining regions of a freely-expanding plasma generated by a cascaded arc. This plasma source can be applied in the field of light source technology,[23] deposition devices[24] and particle sources which are important in thermonuclear research.[25] For a successful application of the cascaded arc and from a fundamental point of view, the physical state of the plasma has to be understood. It has been the subject of a large number of investigations.[22,26,27] In the study of Timmermans et al[26] and the CR-model calculations of Vlček and Pelikán and references therein,[22] the nonequilibrium processes in the cascaded arc are investigated. Typical plasma parameters in the high pressure cascaded arc are electron densities of $n_e = 10^{21} \sim 2 \times 10^{23}\,\mathrm{m}^{-3}$, neutral particle densities of $n_1 = (0.2 \sim 1) \times 10^{24}\,\mathrm{m}^{-3}$ and $T_e \simeq 10000$ K.[28]

Studies of Kimura et al[28] and Limbaugh[29] were devoted to the elucidation of nonequilibrium and non-ideal effects in the freely expanding plasma jet. Recent spectroscopic measurements of van de Sanden[30] supplied us with reliable data of the local plasma parameters at various positions in the expanding plasma jet. Values for the plasma parameters at axial positions $z/D > 4$ from the exit of the cascaded arc, where z is the distance to and D is the diameter of the arc orifice, are $n_e < 10^{20}\,\mathrm{m}^{-3}$, $n_1 \leqslant 10^{21}\,\mathrm{m}^{-3}$ and $T_e \leqslant 3500$ K. The measurements were performed with an arc current of 45 A and an argon flow of 58 scc/sec. The plasma flows through an orifice of $D = 4$ mm and the low pressure background is about 40 Pa.

4. RESULTS

4.1. The atomic state distribution function

In this subsection the experimental results of Ref. 30 will be used to study the influence of the rate coefficients, radiative decay and radiation trapping on the ASDF of an expanding plasma jet. The expanding plasma jet is a low temperature argon plasma with relatively high n_e values (cf. Table 1). Only for the $4s$ and $4p$ levels will the radiative decay compete with the electron-induced transitions. For higher states the electron-induced deexcitation process will be dominant. These levels are in the so-called deexcitation saturation balance:[4] the level population $n(p)$ is a result of balance between deexcitation of higher levels giving rise to production of $n(p)$ and deexcitation from p to lower levels.

Table 1. Values of electron temperature (K), electron and neutral particle densities at various axial (Z) and radial (R) positions in the expanding plasma arcjet. The notation 4.4^{19} means 4.4×10^{19}.

	R = 0 mm			R = 9 mm		
Z (mm)	$T_e(K)$	$n_e(m^{-3})$	$n_1(m^{-3})$	$T_e(K)$	$n_e(m^{-3})$	$n_1(m^{-3})$
20	1800	4.4^{19}	9^{20}	2000	2.9^{19}	7^{20}
40	2400	1.7^{19}	2.2^{20}	2300	2.1^{19}	4.2^{20}
70	3000	3.7^{19}	6.6^{20}			

A level p, for which the condition $p > \max(p_{cr}, p_{hc})$ holds, will be populated according to Eq. (9). The lower lying levels have to be calculated with the hybrid cut-off technique, taking apart from the electron-induced transitions the effect of radiation and radiation trapping into account. In the calculations, 46 effective levels are included which corresponds to a cut-off at pqn $N = 13$. In the CR-model all $4p$ and $4p'$ levels have been lumped into one effective $4p$ level.

Table 1 gives an overview of the local values of the plasma parameters in the expanding plasma jet for which the CR-model is applied. The axial positions $z = 20$ and 40 mm correspond to positions before and in the shock front, while the position at $z = 70$ mm is located behind the shock front. Line-emission measurements are used to determine the population densities $n(p)$ of the excited states listed in Table 2. A tomographic technique is used to Abel invert the lateral profiles. The accuracy of the $n(p)$-values thus obtained is better than 25% for the $4p$-levels, while for the higher lying levels it is, due to the uncertainty in the A-value rather poor, say a factor 2. The Saha-values $n^S(p)$ are obtained using n_e and T_e values which are determined by a Thomson–Rayleigh scattering set-up.[30] With this technique where the scattered photons are dispersed over more than a hundred pixels of an intensified optical multichannel analyzer an accuracy in n_e and T_e is reached within 7%. The Rayleigh scattering is used to get the ground-state density. This n_1 value is needed to calculate the escape factor for the radiative decay of the $4s$ levels to the ground-state. The uncertainty in $b(p) = n(p)/n^S(p)$ for higher levels is mainly determined by the inaccuracy in $n(p)$ while for lower levels the error in T_e will effect $n^S(p)$ via the factor $\exp(E_{p+}/kT)$. This means that an error in $b(p)$ of a factor 2 is typical for the whole p-range.

In Figs. 1(a–e), where $b(p)$ vs p is shown, the results of the hybrid model are compared with the experimental results obtained at the locations given in Table 1. To investigate the influence of

Table 2. Spectral lines of Ar I used in the measurement, E_{p+} (eV) is the ionization energy, λ the wavelength of the transition and g_p the statistical weight of the upper level.

spectroscopic notation	λ (nm)	E_{p+} (eV)	g_p
4p[5/2]	811.5	2.69	7
4p[3/2]	763.5	2.59	5
4p´[1/2]	696.5	2.44	3
4p´[1/2]	750.4	2.275	1
5p[1/2]	419.8	1.265	1
5p[3/2]	420.1	1.185	7
4d[1/2]	693.8	1.065	1
6s[3/2]	703.0	0.915	5
4d´[3/2]	591.2	0.755	3
7s[3/2]	588.9	0.575	5
5d´[3/2]	518.8	0.455	5

the rate coefficients two different sets of rate coefficients were used. The results of the set of Vriens and Smeets are denoted by V, those using Drawin are denoted by D (full lines).

It turns out that for all positions the $b(p)$-factor for the lower lying levels is much smaller than 1, which indicates that the expanding plasma jet is in a non-equilibrium recombining state. It is also observed that for both cases V and D the value $b = 1$ is approached which supports the statement that higher lying levels are in pLSE. Moreover, as indicated by the quantity δb depicted at the right hand side of the Figs. 1(a–b), it is shown that the approach of pLSE obeys the relation $\delta b \propto p^{-6}$ for both cases V and D. This justifies the cut-off technique.

In general, the ASDF using Drawin rates turn out to have higher b-values. This is related to the fact that especially for low T_e-values the rates for highly excited states of D may exceed those of V by more than a factor 60, while deexcitation rates of the lower levels are in both variants dictated by the values of experimental values of Tachibana.[13]

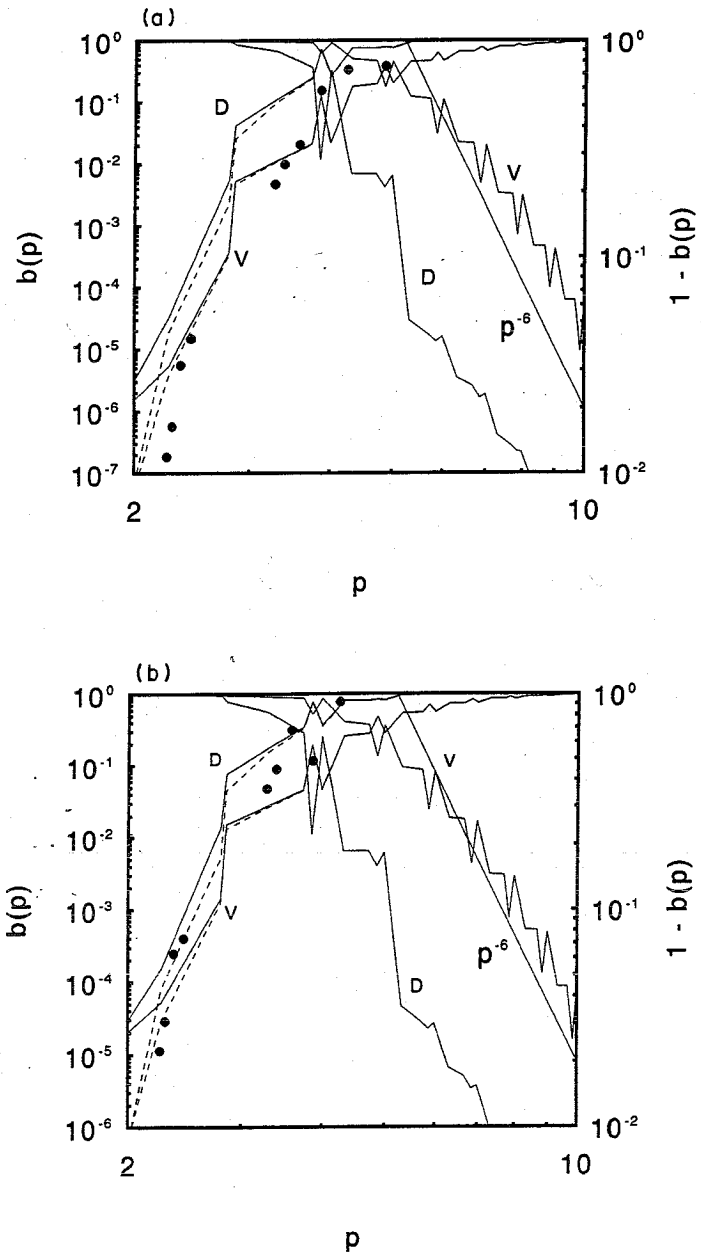

Fig. 1(a) and (b). *Caption on facing page.*

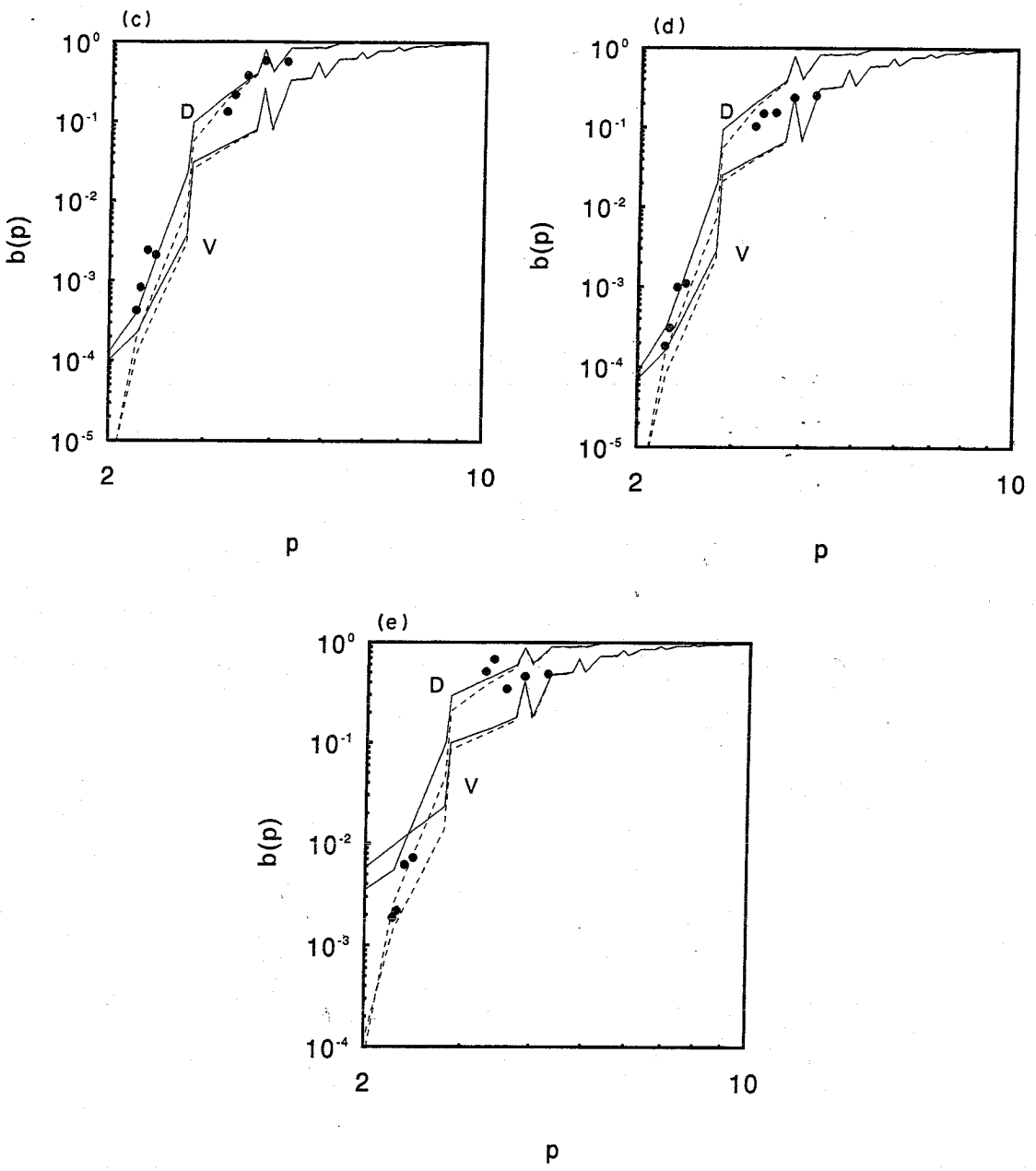

Fig. 1. The $b(p)$ factor vs p taking radiation trapping into account (———) and optically-thin plasma (– – –); ● experimental values of van de Sanden.[30] On the right axis, the p^{-6} dependence of $1 - b(p)$ obtained by the model is investigated for highly excited levels. The curves denoted by V are obtained with rate coefficients of Vriens and Smeets[9] and those denoted with D are obtained with rate coefficients of Drawin.[10] (a) $Z = 20$ mm and $R = 0$ mm, (b) $Z = 20$ mm and $R = 9$ mm, (c) $Z = 40$ mm and $R = 0$ mm, (d) $Z = 40$ mm and $R = 9$ mm, (e) $Z = 70$ mm and $R = 0$ mm.

Comparison shows there is a tendency that the density of the lowest $4p$ level is lower than the lowest model result (model V), with an important exception at the center of the shock. This might suggest that the depopulation of $4p$ is larger than predicted by the models. Probably there is an extra depopulation process not included in our model which is not operative in the shock. To investigate the influence of radiation trapping we used both variant V and D to calculate the ASDF for an optically thin plasma putting $\Lambda = 1$ (broken curves). It turns out that the effect of radiation trapping on the calculated Saha-decrement is only substantial for the lower lying levels. The lowering of the $4p$ group is due to the radiative decay of the higher lying levels $3d$ and $5s$. The occupation of the $4s$ level appears to be of no influence on that of the $4p$ level. It can be seen that

there is a reasonable agreement between the measurements and the optically thin model *V*. Again, this is not true for the shock position for which the optically thick model *D* gives a good fit of the experimental results.

4.2. Recombination coefficient

The total recombination rate coefficient α_{cr} defined such that $n_e n_+ \alpha_{cr}$ represents the number of recombination processes per unit of volume and time is an important parameter in modeling flowing plasmas. The explicit expressions for α_{cr} in terms of the r^+ coefficients as given in Refs. 1, 3 and 4,

$$\alpha_{cr} = \sum_{q \geq 1} \{n_e K_+(q) + A(+,q)\} - \sum_{q>1} n^S(q) r^+(q) S(q)/n_+, \tag{10}$$

makes it possible to use the numerical calculated ASDF to compute α_{cr}. In the above equation $K_+(q)$ and $A(+,q)$ are the rate coefficients for three-body and radiative recombination, respectively, whereas $S(q)$ is the rate coefficient for ionization. Each summation contains only levels for which the effective *pqn* is smaller than that of the cut-off level. The recombination to the cut-off level can be increased with the stepwise recombination flow in the way as described in Ref. 4. This is the basis of the conductive cut-off technique. In the high n_e-limit, radiative processes will be unimportant such that α_{cr} scales with n_e [cf. Eq. (10)]. Therefore it is useful to introduce the parameter $\kappa_+ = \alpha_{cr}/n_e$, the total three-body recombination rate coefficient, to study collisional-dominated recombination. In various studies it is argued that for low T_e the electron excitation kinetics can be expressed in terms of E/kT_e solely. The simplest approach is that given by Thomson which for a hydrogenic system predicts,[4,20]

$$\kappa_+ = 2.6 \times 10^{-39} \hat{T}_e^{-4.5}, \tag{11}$$

where $\hat{T}_e$ is expressed in eV. Note that κ_+ does not depend on n_e. It refers to a situation where the whole atomic system is dominated by the cold DSB. Calculations in Refs. 4, 20 and 21 showed the same temperature dependence of the three-body recombination coefficient and are confirmed experimentally by Hinnov and Hirschberg in recombining helium plasmas.[31] For a comparison with experimental κ_+ values for various metals we refer to Refs. 4 and 21. There it is found that Eq. (11) reproduces experimental results within a factor two.[4] A general observation in these works is that the experimental values are higher.

The simple formula Eq. (11) for κ_+ will serve as a guideline in the discussion of the numerically calculated α_{cr} for which we should keep in mind that its validity region is limited to low T_e and high n_e-values. Two series of κ_+ values will be discussed. The first one (cf. Fig. 2), denoted by case *V* is obtained employing Eq. (10) to the r^+ values of a CR model based on rates of $[V + S]$. The second series is obtained using the rate coefficients of Drawin (case *D* cf. Fig. 3). In both cases, we consider κ_+ vs T_e for an optically thin plasma with $n_1 = 10^{20}\,\mathrm{m}^{-3}$ and $n_e = 10^{17}$, 10^{18}, 10^{19}, 10^{20}, $10^{21}\,\mathrm{m}^{-3}$.

First we will investigate the influence of the cut-off technique on the recombination coefficient. Figure 2 shows case *V* based on 26 effective levels which corresponds to a cut-off level with *pqn* $N = 8$. The full line represents calculations with the conducting cut-off. The broken lines refer to a stagnation cut-off, i.e. the coupling between the highest level with the continuum is effected by direct ionization/recombination solely. The full curve lies above the broken one especially for $T_e < 0.3\,\mathrm{eV}$. This is based on the fact that the deexcitation flow and thus the effective stepwise recombination over the cut-off boundary is rather high. If the calculations are done using 46 effective levels it is found that the broken line moves upwards while the full curve is unaltered. The same observation was found for case *D* for both cut-off methods.

To conclude, we may state that the conductive cut-off method is successful in reducing the number in the atomic system especially in the low temperature range. It is a robust technique and independent of the set of rate coefficients.

The dashed-dotted lines in Figs. 2–3 depict Eq. (11). As stated before, this value of κ_+ is obtained for a completely collisional dominated system where recombination is supported by the fact that for free electrons with low temperature deexcitation will dominate over excitation. It is found in both cases *V* and *D* that the κ_+ value approaches a limit for $n_e \to \infty$ which is reached within 1%

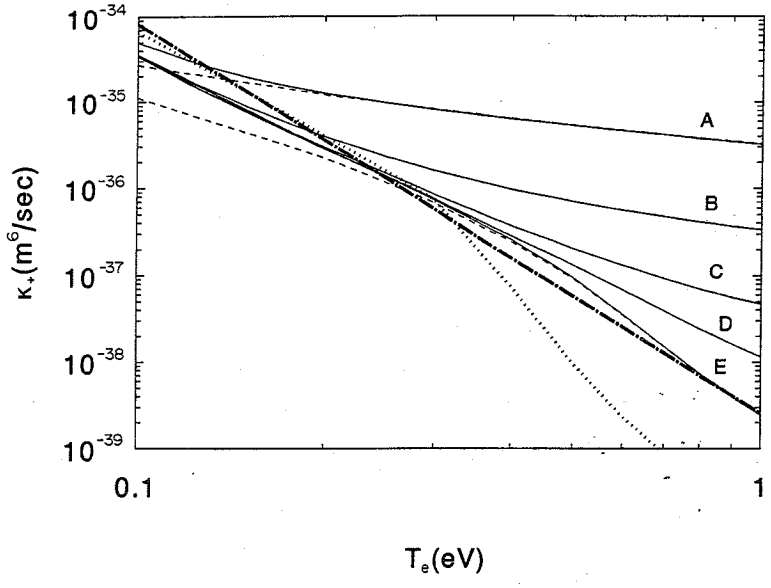

Fig. 2. Recombination coefficient κ_{CR} vs T_e for various n_e and an optically-thin plasma (case *V*). (———): conductive cut-off technique; (– – –): stagnation cut-off technique. (A) $n_e = 10^{17}\,m^{-3}$, (B) $n_e = 10^{18}\,m^{-3}$, (C) $n_e = 10^{19}\,m^{-3}$, (D) $n_e = 10^{20}\,m^{-3}$, (E) $n_e = 10^{21}\,m^{-3}$, (– · – · –): Eq. (11). (· · ·): optically-thick calculation with $n_e = 10^{21}\,m^{-3}$.

for $n_e = 10^{21}\,m^{-3}$ and $T_e = 1$ eV. For lower T_e values, this limit is approached for lower n_e-values. However, comparison shows that the limit values for case *V* and *D* do not coincide with each other nor with the dashed-dotted line (Eq. 11). For low T_e values the κ_+-value of case *V* is a factor 2 too low whereas that of case *D* is factor 1.5 too high. The recombination coefficient scales with $T_e^{-4.2}$ in case *V* while it scales with $T_e^{-4.8}$ for case *D*. This difference between *V* and *D* is related to the different low-T_e behavior of the corresponding rate coefficients. Both semi-empirical cross-section formulae are derived from the Born–Bethe expression, $\sigma_{pq}(E) = [A_{pq}\ln(E/E^*) + B_{pq}]/E$, where the term with A_{pq} represents the optically allowed and the term with B_{pq} the optically forbidden transitions. In the formulae of Drawin $E^* = E_{pq}$ so that the logarithm is always positive[10]

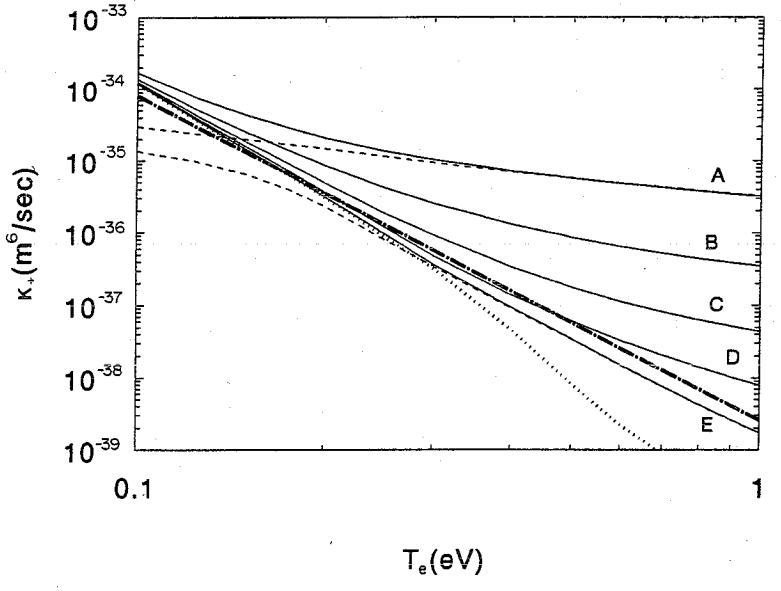

Fig. 3. Recombination coefficient κ_{CR} vs T_e for various n_e and an optically-thin plasma (case *D*). (———): conductive cut-off technique; (– – –): stagnation cut-off technique. (A) $n_e = 10^{17}\,m^{-3}$, (B) $n_e = 10^{18}\,m^{-3}$, (C) $n_e = 10^{19}\,m^{-3}$, (D) $n_e = 10^{20}\,m^{-3}$, (E) $n_e = 10^{21}\,m^{-3}$, (– · – · –): Eq. (11). (· · ·): optically-thick calculation with $n_e = 10^{21}\,m^{-3}$.

while in the formulae of Vriens and Smeets $E^* = 2 \times Ry$ so that this term can be negative at low electron energies and is corrected by the positive B_{pq} term. This results in a reduced cross-section.[9]

Concerning the influence of radiative processes on the recombination, Figs. 2 and 3 reveal that for low T_e-values radiative processes are relatively unimportant. The basic reason is that there is not much competition between radiative decay and the deexcitation processes due to electron collisions, both are downwards. For relatively high T_e-values, we see that radiative processes are important. It is e.g. found for $T_e = 1$ eV and $n_e < 10^{19}$ m^{-3} that κ_+ scales with n_e, i.e. α_{cr} is constant, which means that recombination is essentially determined by the capture-radiative cascade balance, of which the capture processes $e + A^+ \rightarrow A(p)$ is the driving population source.[4]

To study the influence of trapping of radiation we added the κ_+ results based on CR model results in which all the escape factors were set to $\Lambda = 0$ for all resonance transitions and $n_e = 10^{21}$ m^{-3}. This refers to a situation in which the recombination is almost completely controlled by the collisional depopulation of the lower excited states. As indicated by the dotted line in Figs. 2 and 3 it is shown that for $T_e > 0.4$ eV the κ_+ will stay below the value predicted by Eq. (11). This is closely related to the fact that the excitation cross section of Ar is much smaller than that of H. Therefore the same applies to the deexcitation rate. However for decreasing T_e the influence of the $n(4s)$ and $n(3d)$ on the rest of the system will become unimportant and the recombination flow will be controlled to the upper part of the system which is essentially H-like. So the discrepancies between case V, case D and Eq. 11 are not due to the fact that we are dealing with Ar instead of H but due to the fact that the hydrogenic rate coefficients are questionable for low T_e values. This is closely related to the unknown threshold behavior of excitation cross sections.

5. CONCLUSIONS

The hybrid cut-off technique developed in Ref. 3, where it was successfully applied to ionizing systems, is applied to recombining systems. We can draw the following conclusions: (1) the conductive cut-off method is also valid for recombining systems. This is justified by the fact that the quantity δb scales with p^{-6} so that the number of levels in the CR-model can be reduced in a recombining plasma as well. (2) The experimental ASDFs of a cold recombining plasma in an expanding arc jet as measured by van de Sanden[30] lie between the ASDF calculated with case V and D in most cases, but are not able to differentiate between sets of rate coefficients as given by Vriens and Smeets[9] and Drawin.[10] Only the calculated $4p$ level overestimates the lowest experimental $4p$ levels, except at the shock position. This suggests there might be an extra depopulation process of $4p$ which is not included in our model. (3) Since the effective recombination is determined by the upper part of the level system, an accurate description of the excitation flow in the upper part is required which is accomplished by using the conducting cut-off technique. (4) In the limit of high n_e, the recombination coefficient scales with $T_e^{-4.2}$ and $T_e^{-4.8}$ for case V and D, respectively, while $T_e^{-4.5}$ is expected. This difference is caused by different threshold behavior of the cross-section according to Drawin and to Vriens and Smeets.

REFERENCES

1. T. Fujimoto, *J. Phys. Soc. Jap.* **34,** 216 (1973).
2. S. I. Braginskii, in *Reviews of Plasma Physics* Vol. 1, p. 205, M. A. Leontovich ed., New York, NY (1965).
3. D. A. Benoy, J. A. M. van der Mullen, B. van der Sijde, and D. C. Schram, *JQSRT* **46,** 195 (1991).
4. J. A. M. van der Mullen, *Phys. Rep.* **191,** 109 (1990).
5. B. van der Sijde, J. A. M. van der Mullen, and D. C. Schram, *Beitr. Plasmaphys.* **24,** 447 (1984).
6. S. Nowak, J. A. M. van der Mullen, B. van der Sijde, and D. C. Schram, *JQSRT* **41,** 177 (1989).
7. J. A. M. van der Mullen, B. van der Sijde, and D. C. Schram, *Phys. Lett.* **A79,** 51 (1980).
8. J. A. M. van der Mullen, B. van der Sijde, and D. C. Schram, *Phys. Lett.* **A96,** 239 (1983).
9. L. Vriens and A. M. A. Smeets, *Phys. Rev.* **A22,** 940 (1980).
10. H. W. Drawin, EUR-CEA-FC-383 report, Fontenay aux Roses (1966).
11. D. R. Bates, A. E. Kingston, and R. W. P. McWhirter, *Proc. R. Soc.* **A267,** 297 (1962).
12. W. Wiese, M. W. Smith, and B. M. Miles, "Atomic Transition Probabilities", NSRDS-NBS 22, Washington, DC (1969).
13. K. Tachibana, *Phys. Rev.* **A34,** 1007 (1986).
14. M. Klein, Ph.D. Thesis, University of California, Berkeley, CA (1969).
15. K. Katsonis, Ph.D. Thesis, University of Paris (1976).
16. H. Greim, *Phys. Rev.* **131,** 1170 (1963).

17. T. Fujimoto, *J. Phys. Soc. Jap.* **47,** 273 (1979).
18. L. M. Biberman, V. S. Vorob'ev, and I. T. Yakubov, *Sov. Phys. Usp.* **22,** 411 (1979).
19. T. Fujimoto, *Phys. Rev.* **A42,** 6588 (1990).
20. L. M. Biberman, V. S. Vorob'ev, and I. T. Yakubov, *Sov. Phys. Usp.* **15,** 375 (1973).
21. P. Mansbach and J. Keck, *Phys. Rev.* **181,** 275 (1969).
22. J. Vlček and V. Pelikán, *J. Phys. D.* **23,** 526 (1990).
23. A. T. M. Wilbers, G. M. W. Kroesen, C. J. Timmermans, and D. C. Schram, *JQSRT* **45.** 1 (1991).
24. G. M. W. Kroesen, D. C. Schram, and J. C. M. de Haas, *Plasma Chem. Plasma Proc.* **10,** 531 (1990).
25. M. J. de Graaf, R. P. Dahija, J. L. Jeauberteau, F. J. de Hoog, M. J. F. van de Sande, and D. C. Schram, *Coll. Phys.* **18,** C50387 (1990).
26. C. J. Timmermans, R. J. Rosado, and D. C. Schram, *Z. Naturf.* **A40,** 810 (1985).
27. K-P. Nick, J. Richter, and V. Helbig, *JQSRT* **32,** 1 (1984).
28. A. Kimura, K. Tanaka, and M. Nishida, *Rarefied Gas Dynamics*, 1155, S. S. Fischer ed. (1980).
29. C. C. Limbaugh, *Rarefied Gas Dynamics*, 933, J. L. Potter ed. (1976).
30. M. C. M. van de Sanden, Thesis, Eindhoven University of Technology (1991).
31. E. Hinnov and J. Hirschberg, *Phys. Rev.* **125,** 795 (1962).